Valence band offset in heterojunctions between crystalline silicon and amorphous silicon (sub)oxides (a-SiOx:H, 0 x

M. Liebhaber, M. Mews, T. F. Schulze, L. Korte, B. Rech, and K. Lips

Citation: Applied Physics Letters **106**, 031601 (2015); doi: 10.1063/1.4906195
View online: http://dx.doi.org/10.1063/1.4906195
View Table of Contents: http://scitation.aip.org/content/aip/journal/apl/106/3?ver=pdfcov
Published by the AIP Publishing

Valence band offset in heterojunctions between crystalline silicon and amorphous silicon (sub)oxides (a-SiO$_x$:H, 0 < x < 2)

M. Liebhaber,[a] M. Mews,[a] T. F. Schulze, L. Korte,[b] B. Rech, and K. Lips
Institute Silicon Photovoltaics, Helmholtz-Zentrum Berlin für Materialien und Energie, Kekuléstr. 5, D-12489 Berlin, Germany

(Received 28 October 2014; accepted 6 January 2015; published online 20 January 2015)

The heterojunction between amorphous silicon (sub)oxides (a-SiO$_x$:H, $0 < \mathbf{x} < 2$) and crystalline silicon (c-Si) is investigated. We combine chemical vapor deposition with *in-system* photoelectron spectroscopy in order to determine the valence band offset ΔE_V and the interface defect density, being technologically important junction parameters. ΔE_V increases from ≈0.3 eV for the a-Si:H/c-Si interface to >4 eV for the a-SiO$_2$/c-Si interface, while the electronic quality of the heterointerface deteriorates. High-bandgap a-SiO$_x$:H is therefore unsuitable for the hole contact in heterojunction solar cells, due to electronic transport hindrance resulting from the large ΔE_V. Our method is readily applicable to other heterojunctions. © *2015 AIP Publishing LLC*.
[http://dx.doi.org/10.1063/1.4906195]

The interface between crystalline silicon (c-Si) and silicon oxides is of profound interest due to its numerous applications in microelectronics and energy conversion devices. Stoichiometric silicon dioxide is mainly used for surface passivation of c-Si[1] or as gate dielectric in field-effect transistors.[2] In the field of solar energy conversion, there are concepts of current interest which employ a silicon oxide/crystalline Si interface. High-bandgap amorphous Si alloys are potential emitter layers for amorphous/crystalline Si heterojunction (SHJ) solar cells. One suitable model system to study the band lineup in this kind of junction is hydrogenated amorphous silicon oxide (a-SiO$_x$:H). The SHJ technology yields a very high open circuit voltage due to the excellent Si surface passivation enabled by undoped amorphous silicon (a-Si:H) and the full-area passivated contact consisting of doped a-Si:H layers and a transparent conductive oxide.[3,4] A drawback of this approach is a comparably high current loss due to parasitic absorption in the a-Si:H layers.[5,6] An approach to minimize these losses is to use high-bandgap amorphous or microcrystalline Si alloys as passivation and carrier-collection layers.[7–9] Ultrathin (sub)oxides can further be employed as tunneling layers in passivated contact architectures such as semi-insulating polycrystalline Si ("SIPOS") contacts.[10]

For photovoltaic applications, allowing to extract charge carriers from the c-Si absorber while at the same time providing excellent surface passivation defines the functionality of the thin oxide layer. Carrier transport occurs either by tunneling (T) through or by thermionic emission (TE) across the barrier posed by the band offsets. For both transport mechanisms, the valence band offset (ΔE_V) between c-Si and a-SiO$_x$:H is crucial as it defines the barrier height for hole extraction (cf. Fig. 1). Note that a large band offset is not always detrimental. It can also be exploited to selectively block the extraction of one charge carrier type, thus resulting in carrier-selective contacts.[11] However, recent experiments and simulations on suboxide passivation layers for (n)c-Si-based SHJ solar cells have suggested that the expected increase of ΔE_V at the a-SiO$_x$:H/c-Si interface for increasingly oxidic layers is detrimental to the device functionality. Increasing ΔE_V was surmised to be responsible for a deteriorating solar cell fill factor by impeding hole extraction,[7] as visualized in Fig. 1. No systematic study of ΔE_V at the a-SiO$_x$:H/c-Si interface is available in the literature.

The aim of this letter is to provide such a study for a-SiO$_x$:H layers covering the entire range of O contents from zero to a stoichiometric oxide, while at the same time monitoring the electronic quality of the heterointerface relevant for c-Si passivation. We combine state-of-the-art plasma-enhanced chemical vapor deposition (PECVD) of a-SiO$_x$:H with *in-system* photoelectron spectroscopy (PES) for the determination of valence band (VB) offsets in device-relevant structures, which is readily applicable also to other hetero-contact materials.[12]

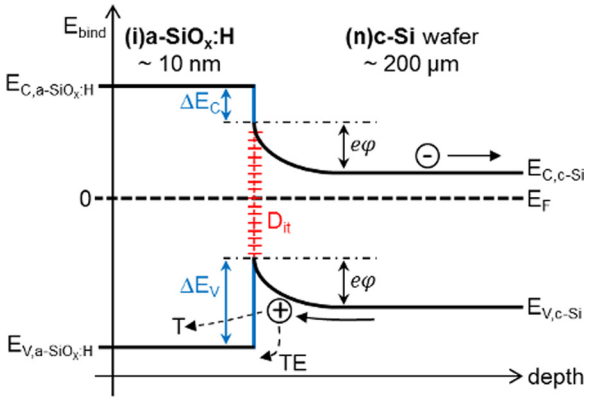

FIG. 1. Schematic of the a-SiO$_x$:H/c-Si band lineup, relevant physical quantities, as well as possible extraction paths for holes by tunneling (T) and thermionic emission (TE). In order to determine the VB offset ΔE_V, the band bending $e\varphi$ is measured by the SPV technique,[12] while the a-SiO$_x$:H VB position (relative to E$_F$) is determined by PES. The c-Si VB position E$_{V,c\text{-}Si}$ is known from the c-Si doping. For SPV, flat bands in the (i)a-SiO$_x$:H are assumed, since the excitation laser pulse energy is below the a-Si:H bandgap, hence, no photogeneration occurs in this layer.

[a]M. Liebhaber and M. Mews contributed equally to this work.
[b]Author to whom correspondence should be addressed. Electronic mail: korte@helmholtz-berlin.de

In our study, we used 200 μm thick (111)-oriented 0.5–1 Ω cm phosphorus-doped high quality float zone Si wafers as substrate material. Prior to deposition, the wafers were cleaned following the RCA cleaning procedure and dipped in diluted hydrofluoric acid (1%, 2 min) to strip off the native silicon oxide. Depositions were done in a conventional parallel plate PECVD at 60 MHz excitation with 55 mW/cm^2 power density at 175 °C and 0.5 mbar chamber pressure using $SiH_4/H_2/CO_2$ precursor gas mixtures. In order to grow a-SiO_x:H layers with varying x, SiH_4, and CO_2 gas flows adding up to a total of 10 sccm were employed at a constant H_2 flux of 5 sccm, while varying the ratio $R = CO_2/SiH_4$ from 0 to 4. Layer thicknesses and bandgaps of the a-SiO_x:H layers were determined by spectroscopic ellipsometry on a Sentech SE850 (wavelength range 190–850 nm), followed by fitting of a Tauc-Lorentz model[13] to the data. The bandgap of the layers showed a significant widening upon O incorporation, starting from the a-Si:H value of 1.7 eV and rising up to ≈3 eV for near-stoichiometric a-SiO_2. This is in accordance with earlier studies,[14] which revealed that the bandgap values of a-SiO_x:H (higher-x regime) are drastically underestimated by optical measurements and seemingly saturate at about 3 eV for stoichiometric oxides, due to band tail absorption. Minority carrier lifetime measurements were conducted using a commercial photoconductance decay (PCD) setup.

Central to the study was the determination of the VB edge position as well as the stoichiometry of the a-SiO_x:H layers, with different modes of PES. To this end, 10 nm thick a-SiO_x:H layers were grown on c-Si and transferred from the PECVD to an ultrahigh vacuum analysis chamber via a vacuum transfer system. X-ray PES (XPS) was performed using Mg K_α radiation from a conventional X-ray source (SPECS Nano Surface Analysis GmbH), in order to quantify the a-SiO_x:H stoichiometry. Near-ultraviolet PES measurements using a high pressure Xe lamp and a double grating monochromator providing photon energies between 4.0 and 7.3 eV were conducted in the constant-final-state-yield mode (CFSYS).[15] The VB tail and edge position were determined by fitting a model density of states (DOS) to the data.[16] For the layers deposited with $R \geq 1$, the excitation energy of 7.3 eV in the CFSYS mode was not sufficient to excite photoelectrons from the VB edge to the vacuum in order to be detected. We therefore also measured ultraviolet PES (UPS) using a Helium lamp (He I discharge line at 21.2 eV excitation energy). Band edge positions were extracted by linear extrapolation of the leading edge of the extended states in the model DOS to zero.[16] To quantify the c-Si band bending in equilibrium, we employed the surface photovoltage (SPV) method.[12]

We begin with an analysis of the a-SiO_x:H stoichiometry based on the XPS data. Fig. 2(a) shows the development of the Si 2p peak upon variation of the precursor gas flows, which reflects the changes in the chemical environment of the Si atoms. Upon increasing the CO_2 flow, the dominant Si 2p peak indicative of Si with oxidation state zero is gradually reduced, while a second peak appears on the higher binding energy side between 101 and 104 eV. Indeed, the 2p core level signals for the Si oxidation states 1+…4+ are found in this energy range, and the XPS spectra can be fitted using

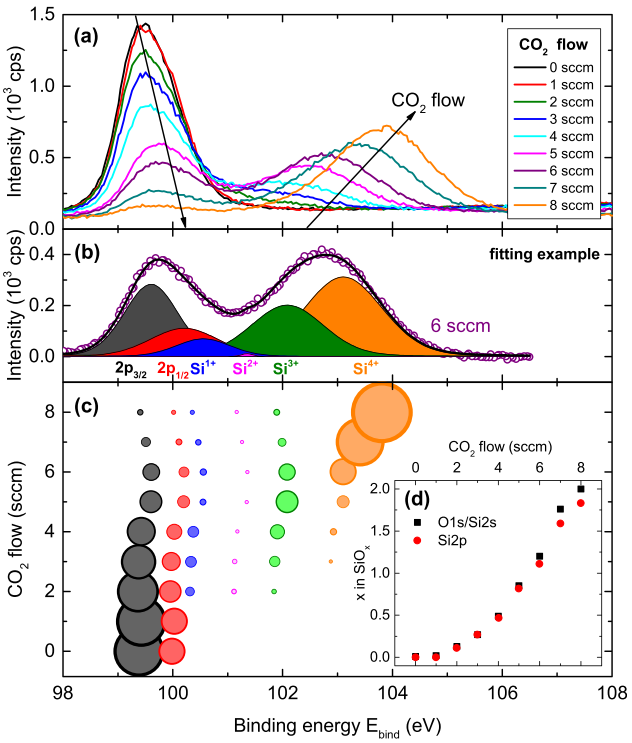

FIG. 2. (a) XPS spectra of a-SiO_x:H layers deposited with different SiH_4/CO_2 flow rates. (b) Exemplary fit (6 sccm CO_2 flow) showing the different Si oxidation states. The composition and shift of the Si 2p peak indicate pronounced changes in the Si chemical environment upon O incorporation. (c) Peak fitting results for the XPS spectra in dependence of the CO_2 flow: Binding energies (symbol position) and areas (symbol size) of the peaks corresponding to different Si oxidation states. (d) Stoichiometry calculated from the XPS analysis using either the ratio of the O 1s to the Si 2s peak area (black squares) or the relative contributions of the Si oxidation states to the Si 2p peak (red points), in dependence on the CO_2 flow during layer deposition.

tabulated peak positions for the different Si oxidation states (example fit shown in Fig. 2(b)). Based on the ratio of the peak areas shown in Fig. 2(c), we can calculate the O to Si ratio of the films, and thus relate the parameter R of the CO_2 flow to the resulting stoichiometry x. Note that this procedure is well-established in literature.[17,18] In Fig. 2(d), we plot the resulting calibration curve of the a-SiO_x:H stoichiometry x vs. CO_2 flow based on this analysis (red symbols). The black symbols mark the results of a complementary method based on the comparison of the O 1s and Si 2s peak weights,[19] yielding comparable results. Thus, the CO_2 flow regime explored here covers the range from pure a-Si:H to nearly stoichiometric a-SiO_2. Based on the XPS data, the C concentration stayed well below 3% of the O concentration for all layers.

In a next step, we assess the changes in the VB structure of the a-SiO_x:H layers upon varying the O content x. Fig. 3 shows an overview of the near-ultraviolet PES and UPS spectra. The spectra for the low-x samples show the typical a-Si:H DOS signature, which has been discussed and evaluated earlier:[16] The VB, at $E_{bind} \approx 2.5$–1 eV in Fig. 3(a), extends into an exponentially decaying VB tail ($E_{bind} \approx 1$–0.75 eV) which merges into a broad distribution of midgap dangling bond (DB) defects ($E_{bind} \approx 0.75$–0 eV). At the Fermi edge ($E_{bind} = 0$ eV), the DB signal is cut off smoothly due to experimental broadening, caused by the

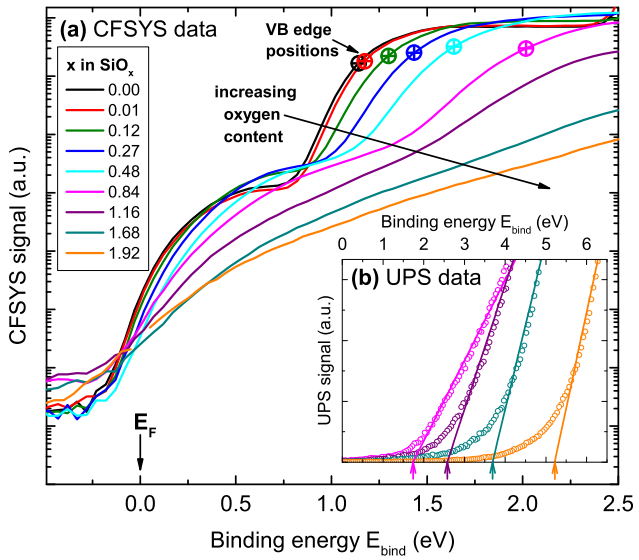

FIG. 3. CFSYS (a) and UPS (b) measurements of the VB DOS for amorphous Si suboxides with different O contents. Starting from a typical a-Si:H DOS featuring a broad distribution of dangling bonds and an exponentially decaying band tail, the DOS develops by a shift of the VB edge to higher binding energy and a flattening of the VB tail. The dots in (a) denote the position of the VB edge as obtained by fitting a model DOS to the CFSYS data, while a linear extrapolation is employed for the UPS data in (b), and arrows mark the obtained band edge.

finite resolution of the excitation source and energy analyzer. As seen in Fig. 3, the VB edge shifts to higher binding energies for increasing x, while the VB tail is getting shallower. It appears that the amplitude of the DB-related peak increases before it saturates, while its width steadily increases. The net result is a steady increase of DB density for increasing x, consistent with the increasing density of strained bonds manifesting in the VB tail (cf. Fig. 4(b)).[20] Thus, the electronic quality of the a-SiO_x:H layers deteriorates with increasing x. For the highest x values, a reliable determination of the VB edge is impossible using CFSYS as

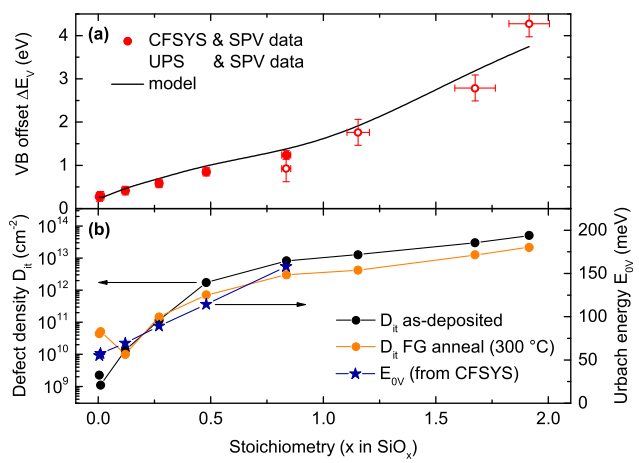

FIG. 4. (a) Development of the a-SiO_x:H/c-Si VB offset ΔE_V derived from combining PES and SPV data, upon varying the O fraction in the layers. The black line is the prediction by a simple rigid-band-model based on the effective Si 2p peak shifts and the changing H density. (b) Interface defect density D_{it} (left axis) as deduced from PCD measurements and Urbach energy E_{0V} (right axis) observed in the CFSYS data, marking the deterioration of a-SiO_x:H bulk electronic quality upon increased O incorporation.

the VB has shifted towards higher binding energies beyond the range accessible with our UV lamp. However, using He-UPS, we can still observe the VB edge and track its further evolution, while lacking the signal-to-noise to resolve VB tail or DBs (Fig. 3(b)). The marks on the CFSYS curves of Fig. 3(a) show the E_V values obtained by fitting a model DOS,[16] while the linear extrapolation of the He-UPS band edges employed for $x \geq 0.8$ is shown in the inset. For $x = 0.84$, we applied both methods for the determination of the VB edge and found agreement within 0.3 eV. These 0.3 eV are a good estimate for the systematic error in determining E_V from our PES data.

In order to determine ΔE_V, we need to further consider possible changes of the *equilibrium band bending* in the heterostructure (cf. Fig. 1). We therefore measure the band bending $e\varphi$ using the SPV technique on the PES samples immediately after removal from the ultrahigh vacuum system. We find $e\varphi < 0.15$ eV for all the samples, resulting in a nearly 1-to-1 correspondence of the energetic retreat of the VB edge relative to E_F to the changes in ΔE_V. Fig. 4(a) shows ΔE_V calculated by combining PES and SPV data of the a-SiO_x:H/c-Si samples using $\Delta E_V = E_{V,a\text{-}SiOx:H} - E_{V,c\text{-}Si} + e\varphi$ (cf. Fig. 1). We see that starting from $\Delta E_V \approx 0.3$ eV for pure a-Si:H, ΔE_V monotonously increases to reach more than 4.0 eV for near-stoichiometric a-SiO_2.

These results are in line with previous works concerning the *end points* of the stoichiometry series: Van de Walle calculated $\Delta E_V = 0.2$ eV for 11%-hydrogen containing a-Si:H on c-Si,[21] while we have measured in previous studies[12,16] $\Delta E_V = 0.3$–0.45 eV for a-Si:H layers which mostly contained a higher H concentration. Given the wide variety of different possible H microstructures in a-Si:H and the according differences in bandgap, the value obtained here fits well with the existing data. For the stoichiometric a-SiO_2/c-Si heterojunction, $\Delta E_V \approx 4.4$ eV has been established experimentally,[22,23] also in line with our current findings.

Using Fourier transform infrared spectroscopy, we quantified the H content of our layers, which we found to decrease from about 20% to ≈0% within the considered x range, with a particularly steep decrease around $x \approx 0.5$. Thus, from the development of the H content alone, a net *decrease* of ΔE_V would be expected for the considered series, with a magnitude of 0.2–0.5 eV depending on the assumed correlation of the H content with ΔE_V.[12,21] The observed pronounced *increase* of ΔE_V with x by more than 3.5 eV thus proves that the O content is the main driver for ΔE_V in the samples considered here. While the general trend of a monotonous increase of ΔE_V from the values accepted for a-Si:H/c-Si to the a-SiO_2/c-Si values observed here seems logical, it is worthwhile to compare our results to a basic model: We invoke the naïve idea of a rigid-band-model (as is often used for c-Si),[24] assuming that the shift of the Si 2p core levels observed with XPS translates into a concomitant shift of the VB edge, while taking into account the compensating role of H removal alongside O incorporation. We calculate the effective Si 2p core level shift from the data in Fig. 2, averaging over the different oxidation states' individual shifts, while taking the XPS peak area as the weighting factor for the averaging. The impact of the H content on ΔE_V is assumed to be 13 meV/at. %, as we have previously

measured on a-Si:H.[12] Thus, we can estimate the expected retreat of the VB edge resulting from the Si 2p core level shift. Obviously, this picture may break down at some point for high x as the VB top of a-SiO_2 consists of oxygen-derived states,[25] while for a-Si:H, it is derived from Si p-orbitals. Nonetheless, we observe a promising agreement of our rather basic model (black line in Fig. 4(a)) with the measured ΔE_V values.

Now, we turn to the analysis of the a-SiO_x:H passivation behavior. We fabricated double-side polished c-Si wafers symmetrically passivated with 10 nm of the layers studied above, measured PCD and fitted the data with a semi-empirical model describing interface recombination[26] to extract the interface defect density D_{it}. The resulting D_{it} values for the as-deposited state as well as after a subsequent 300 °C forming gas (H_2/N_2) anneal are plotted vs. x in Fig. 4(b). Obviously, the passivation quality starts from an excellent level at $x = 0$ and decreases for larger x. A forming gas anneal is detrimental for low-x values, while it decreases D_{it} by up to an order of magnitude for higher x, consistent with previous studies on PECVD-grown a-SiO_2,[27] albeit on a low level. This indicates suboptimal deposition parameters in the high-x range regarding the resulting interface quality. The observed trend in defect density is consistent with the decreasing VB tail slope (corresponding to an increasing Urbach energy, plotted as stars in Fig. 4(b))[20] and the idea that D_{it} is closely related to the bulk defect density in the amorphous film.[28] The observed gradual H removal from the films with increasing x likely contributes to higher strain/disorder and thus increased bulk defect density in the a-SiO_x:H[29] via the conversion of strained bonds into dangling bonds,[30] manifesting in deteriorated interface passivation.

Finally, we discuss the implications of our obtained results on ΔE_V and D_{it} for the application of a-SiO_x:H films in high-efficiency Si solar cells. Modeling studies have identified 0.4–0.6 eV as a critical threshold value for ΔE_V of (n)c-Si based solar cells, above which the hole extraction via thermionic emission is beginning to limit the solar cell performance by reduction of the fill factor.[31,32] Although the exact value of said threshold depends on the tunneling mechanisms considered, and on the density of VB tail states serving as final states for tunneling processes, there is general agreement on the existence and approximate range of such critical ΔE_V. Furthermore, experimental studies found a deteriorating fill factor of a-SiO_x:H/c-Si solar cells for increasing x,[7] and also reported decreasing passivation properties for oxidic layers.[7,8] This can be explained in the light of our results which suggest that x is restrained to values below 0.2 in order to both avoid critical ΔE_V values and to preserve good passivation properties. However, this limits the a-SiO_x:H bandgap to ≈2.0 eV,[33] which results in only negligible current gain as compared to standard a-Si:H emitters ($E_g \approx 1.7$ eV). Replacing 10 nm a-Si:H—a typical thickness for SHJ solar cell emitters—by a-$SiO_{0.2}$:H, the reduction in parasitic absorption is only roughly 0.4 mA/cm^2 as calculated using our optical data. Thus, it appears that a-SiO_x:H is *not* a candidate for significant current improvement in (n)c-Si based SHJ solar cells because of the rapid increase in ΔE_V upon gap widening. Unfortunately, this physical behavior seems to be a generic feature of a-Si:H-derived alloys as it is also observed for a-Si:H/c-Si with varying H content[12] as well as for a-SiC_x:H/c-Si heterojunctions.[34] In conclusion, this renders the family of a-Si:H alloys to be more promising as an electron-selective contact on a *p-type* Si absorber,[9] but unsuitable for incorporation into the emitter of (n)c-Si absorbers in a standard SHJ emitter concept, as also stated in Ref. 7.

If the higher transparency of near-stoichiometric Si oxides is to be exploited, the device would need to rely on tunneling through an ultrathin layer instead of thermionic transport over a barrier. However, such a contact concept involves a significant challenge regarding the realization of excellent interface passivation, which usually requires elaborate high-temperature processing steps.[10,35] Alternatively, metal oxides as SHJ-emitter materials[36] might provide considerably higher potential for increased current yield on (n)c-Si while preserving good transport properties. Once looking beyond Si alloys, the wide variety of candidates potentially enables a tailored emitter design in order to realize a well-passivated hole-selective contact on (n)c-Si. The analysis method used in this letter will prove useful in the analysis of such Si-based heterojunctions in order to assess their applicability to high-efficiency Si solar cells.

We thank T. Lußky, E. Conrad, K. Jacob, M. Wittig, and K. Holldack for experimental support and F. Ruske for fruitful discussions. Financial support was provided by the German Federal Ministry for Research and Education (BMBF) through the project "Silicon *In-situ* Spectroscopy at the Synchrotron" (SISSY), Grant No. BMBF-03SF0403 and by the European Commission through the FP7-ENERGY Project "HERCULES," Grant Agreement No. 608498.

[1]M. J. Kerr, J. Schmidt, A. Cuevas, and J. H. Bultman, J. Appl. Phys. **89**, 3821 (2001).
[2]S. M. Sze and K. N. Kwok, *Physics of Semiconductor Devices*, 3rd ed. (John Wiley & Sons, Inc., Hoboken, New Jersey, 2007).
[3]M. Taguchi, A. Yano, S. Tohoda, K. Matsuyama, Y. Nakamura, T. Nishiwaki, K. Fujita, and E. Maruyama, IEEE J. Photovoltaics **4**, 96 (2014).
[4]S. De Wolf, A. Descoeudres, Z. C. Holman, and C. Ballif, Green **2**, 7 (2012).
[5]M. Lu, S. Bowden, U. Das, and R. Birkmire, Appl. Phys. Lett. **91**, 063507 (2007).
[6]Z. C. Holman, A. Descoeudres, L. Barraud, F. Z. Fernandez, J. P. Seif, S. De Wolf, and C. Ballif, IEEE J. Photovoltaics **2**, 7 (2012).
[7]J. P. Seif, A. Descoeudres, M. Filipic, F. Smole, M. Topic, Z. C. Holman, S. De Wolf, and C. Ballif, J. Appl. Phys. **115**, 024502 (2014).
[8]K. Ding, U. Aeberhard, F. Finger, and U. Rau, J. Appl. Phys. **113**, 134501 (2013).
[9]D. Pysch, M. Bivour, M. Hermle, and S. W. Glunz, Thin Solid Films **519**, 2550 (2011).
[10]E. Yablonovitch, T. Gmitter, R. M. Swanson, and Y. H. Kwark, Appl. Phys. Lett. **47**, 1211 (1985).
[11]P. Würfel, Physica E **14**, 18 (2002).
[12]T. Schulze, L. Korte, F. Ruske, and B. Rech, Phys. Rev. B **83**, 165314 (2011).
[13]G. E. Jellison and F. A. Modine, Appl. Phys. Lett. **69**, 371 (1996).
[14]A. Janotta, Y. Dikce, M. Schmidt, C. Eisele, M. Stutzmann, M. Luysberg, and L. Houben, J. Appl. Phys. **95**, 4060 (2004).
[15]M. Sebastiani, L. D. Gaspare, G. Capellini, C. Bittencourt, and F. Evangelisti, Phys. Rev. Lett. **75**, 3352 (1995).
[16]L. Korte and M. Schmidt, J. Appl. Phys. **109**, 063714 (2011).
[17]S. Lombardo and S. U. Campisano, Mater. Sci. Eng., R **17**, 281 (1996).

[18]F. J. Himpsel, F. R. McFeely, A. Taleb-Ibrahimi, J. A. Yarmoff, and G. Hollinger, Phys. Rev. B **38**, 6084 (1988).
[19]C. Wagner, L. Davis, M. Zeller, J. Taylor, R. Raymond, and L. Gale, Surf. Interface Anal. **3**, 211 (1981).
[20]M. Stutzmann, Philos. Mag. B **60**, 531 (1989).
[21]C. V. de Walle and L. H. Yang, J. Vac. Sci. Technol., B **13**, 1635 (1995).
[22]J. Keister, J. Rowe, J. Kolodziej, H. Niimi, T. Madey, and G. Lucovsky, J. Vac. Sci. Technol., B **17**, 1831 (1999).
[23]H. Nohira, A. Omura, M. Katayama, and T. Hattori, Appl. Surf. Sci. **123**, 546 (1998).
[24]F. J. Himpsel, G. Hollinger, and R. A. Pollak, Phys. Rev. B **28**, 7014 (1983).
[25]Y.-n. Xu and W. Ching, Phys. Rev. B **44**, 11048 (1991).
[26]C. Leendertz, N. Mingirulli, T. Schulze, J. Kleider, J. Rech, and L. Korte, Appl. Phys. Lett. **98**, 202108 (2011).
[27]Z. Chen, S. Pang, K. Yasutake, and A. Rohatgi, J. Appl. Phys. **74**, 2856 (1993).
[28]T. Schulze, H. Beushausen, C. Leendertz, A. Dobrich, B. Rech, and L. Korte, Appl. Phys. Lett. **96**, 252102 (2010).
[29]G. Cody, T. Tiedje, B. Abeles, B. Brooks, and Y. Goldstein, Phys. Rev. Lett. **47**, 1480 (1981).
[30]M. J. Powell and S. C. Deane, Phys. Rev. B **48**, 10815 (1993).
[31]A. Kanevce and W. K. Metzger, J. Appl. Phys. **105**, 094507 (2009).
[32]M. Rahmouni, A. Datta, P. Chatterjee, J. Damon-Lacoste, C. Ballif, and P. R. i Cabarrocas, J. Appl. Phys. **107**, 054521 (2010).
[33]T. Mueller, S. Schwertheim, M. Scherff, and W. R. Fahrner, Appl. Phys. Lett. **92**, 033504 (2008).
[34]T. M. Brown, C. Bittencourt, M. Sebastiani, and F. Evangelisti, Phys. Rev. B **55**, 9904 (1997).
[35]F. Feldmann, M. Simon, M. Bivour, C. Reichel, M. Hermle, and S. W. Glunz, Appl. Phys. Lett. **104**, 181105 (2014).
[36]C. Battaglia, S. M. De Nicolas, S. M. De Wolf, S. M. Yin, M. Zheng, C. Ballif, and A. Javey, Appl. Phys. Lett. **104**, 113902 (2014).